

A Maximum Entropy Method of Obtaining Thermodynamic Properties from Quantum Monte Carlo Simulations

Carey Huscroft, Richard Gass, and Mark Jarrell
Physics Department, University of Cincinnati, Cincinnati, OH 45221-0011

We describe a novel method to obtain thermodynamic properties of quantum systems using Bayesian Inference – Maximum Entropy techniques. The method is applicable to energy values sampled at a discrete set of temperatures from Quantum Monte Carlo Simulations. The internal energy and the specific heat of the system are easily obtained as are errorbars on these quantities. The entropy and the free energy are also obtainable. No assumptions as to the specific functional form of the energy are made. The use of *a priori* information, such as a sum rule on the entropy, is built into the method. As a non-trivial example of the method, we obtain the specific heat of the three-dimensional Periodic Anderson Model.

PACS numbers: 02.50.Rj, 65.50.+m, 02.70.Lq, 71.45.-d

I. INTRODUCTION

The problem of obtaining thermodynamic properties from Quantum Monte Carlo (QMC) simulations is one of long-standing interest. [1]. Although the internal energy, i.e., the expectation value of the Hamiltonian, is one of the easiest quantities to obtain via QMC, the free energy is almost impossible to obtain directly in a simulation. Likewise, the specific heat, i.e., the temperature derivative of the internal energy, is very difficult to obtain directly. Hence, one must turn to indirect methods.

Several methods to obtain the thermodynamic properties of model systems via QMC have been proposed, but all suffer from limitations of one sort or another. To a large extent, these stem from the use of a specific functional form to fit the internal energy of the system. We propose a novel method to obtain the internal energy, the specific heat, the entropy, and the free energy as a function of temperature via QMC which does not impose any functional form on these quantities and alleviates several other problems in the current methods. Our technique relies on probability theory and Maximum Entropy to obtain the *most probable* thermodynamic functions consistent with the QMC data and prior knowledge, such as a sum rule on the system's entropy.

In the remainder of this paper, Sec. II reviews currently used techniques to obtain thermodynamic properties from QMC, their limitations, and the desirable features of a new technique. Sec. III contains a brief overview of our method to obtain thermodynamic quantities from QMC data. In Sec. IV, we review the theoretical underpinnings of the method, Maximum Entropy. Sec. V sets forth the algorithmic details of our method. In order to test our method, we apply it to a non-trivial problem – the 3d Periodic Anderson Model – in Sec. VI. Our summary is given in Sec. VII.

II. BACKGROUND

The free energy and its derivatives, including the specific heat, provide experimentally relevant insight into a system's temperature evolution and phase transitions. Unfortunately, both direct and indirect QMC measurements of such quantities are notoriously difficult to make. To understand why, we discuss two methods for obtaining thermodynamic quantities in this section.

Typically, one tries to obtain the thermodynamic properties of a system by performing QMC simulations at various discrete temperatures, then fitting the resultant energy data to a functional form. Generally, this functional form is not known, so a physically-motivated form must be chosen. The recipe is to fit the internal energy $E(T)$ to a functional form, which may then be differentiated explicitly to obtain the specific heat

$$C(T) = \frac{\partial E(T)}{\partial T}. \quad (1)$$

From the specific heat, the entropy $S(T)$ may be calculated by integrating

$$S(T) = \int_0^T dT' \frac{C(T')}{T'}. \quad (2)$$

Then, the free energy F may be obtained from the relation

$$F(T) = E(T) - TS(T). \quad (3)$$

While apparently sound in principle, this prescription can manifest several serious problems. For one, the derivative in Eq. 1 enhances the statistical uncertainty in the fit. At low temperatures the procedure is further complicated by the division by T in Eq. 2. Similar problems emerge at low T when the specific heat is evaluated directly $C = (\langle E^2 \rangle - \langle E \rangle^2) / T^2$. Thus, there is no guarantee that the total entropy obtained by this method

$$S_\infty = \int_0^\infty dT \frac{C(T)}{T} \quad (4)$$

will equal the total infinite-temperature entropy of the system. If not, then both the specific heat $C(T)$ and the free-energy $F(T)$ may be unreliable.

One technique using this prescription is to fit QMC internal energy data to a pair of functional forms, one for low-temperature data and another for high-temperature data. [2] This method has been successfully applied, but it does have several important drawbacks. First, separate functional forms in the nature of polynomials are used for the low- and the high-temperature regions. These are chosen after viewing the data, based on the shape of the $E(T)$ curve. Presumably, care must be taken to avoid spurious features in the derivative $C(T)$ of the internal energy $E(T)$ at the point where the two polynomials are joined. While an analytic function such as a polynomial expansion is a reasonable choice for an internal energy function on a finite-dimensional lattice, there is no guarantee that sufficient terms have been chosen for the polynomial and the most reliable test is a goodness of fit. Consequently, this technique requires a great deal of costly QMC data, especially in the neighborhood of a phase transition, in order to insure that a reasonable goodness of fit is obtained.

Another recently-proposed method to obtain thermodynamic properties from QMC data is to fit the internal energy $E(T)$ to a physically-motivated functional form. [3,4] In this method, appropriate for a lattice simulation, the internal energy is fit to a sum of exponentials

$$E(T) = E_0 + \sum_n c_n e^{-n\Delta/T}. \quad (5)$$

The specific heat and the entropy are then obtained according to Eqs. 1 & 2, respectively.

One way to view the exponential functional form of this method is to note that physically, one may expect different energy scales to become important as the temperature T is varied. At those energy scales, contributions to the internal energy $E(T)$ are effectively switched on. This is manifest in the fitting parameter Δ ; at each temperature corresponding to the energy scale $n\Delta$ for each of the n terms in the expansion, another term in the expansion contributes to the energy. The amplitude of this contribution is set by the related coefficient c_n .

This technique has been successfully applied. It has at least one major advantages over the polynomial method in that it does not splice together two functions for different temperature regimes. Nevertheless, it also relies on a goodness of fit test to determine whether a reasonable number of fitting parameters have been chosen. Since it uses a gapped form for the internal energy, it is not suitable for systems in the thermodynamic limit, as may be studied using dynamical mean field techniques. Furthermore, both the polynomial and the exponential fitting

schemes are inaccurate when the number of fitting parameters is small and become ill posed as the number of fitting parameters become large. Thus it is difficult to determine how many coefficients to use.

We now present a method that overcomes these drawbacks and possible pitfalls. Our method incorporates additional *a priori* information that the energy $E(T)$ increases monotonically with the temperature T so that the specific heat is positive definite, $C(T) \geq 0$, and in the form of the infinite temperature entropy S_∞ . Thus it requires less QMC data than either of the functional fitting methods. It performs a search for the most probable energy $E(T)$ given the data and prior information, and therefore removes the question of determining the number of fitting parameters appearing when using the other methods. It is applicable to both finite-dimensional lattice QMC as well as QMC from non-gapped systems.

III. OVERVIEW OF THE NEW TECHNIQUE

We start with the observation that given the appropriate distribution function $K(\beta, \omega)$ relating the energy ω to the inverse temperature $\beta = 1/T$, one can write the internal energy as a weighted integral with a positive-definite weight $\rho(\omega)$

$$E(T) = - \int_{-\infty}^{\infty} d\omega \omega K(\beta, \omega) \rho(\omega). \quad (6)$$

The specific heat is obtained by differentiating

$$C(T) = \frac{\partial E(T)}{\partial T} = - \int_{-\infty}^{\infty} d\omega \omega \frac{\partial K(\beta, \omega)}{\partial T} \rho(\omega). \quad (7)$$

One may then use Eqs. 2 and 3 to obtain the entropy and the free energy, respectively.

The entire problem of obtaining the thermodynamic properties of the system then reduces to that of numerically inverting the integral equation Eq. 6 for the weight $\rho(\omega)$ given noisy QMC data for the internal energy $E(T)$. This is a well-known problem for which there exists a well-developed, powerful technique, the Maximum Entropy Method (MEM). [5] (The MEM is discussed in the next section.) The kernel $K(\beta, \omega)$ corresponds to a blurring function which acts on a spectrum $\rho(\omega)$. Typical blurring functions for a quantum system are the Bose-Einstein and the Fermi distribution functions, as discussed in detail in Sec. IV. [6]

To understand the fundamental difference between other methods and our MEM technique, it is important to understand the questions which the two methods answer. The other methods rely on fitting noisy data to a functional form. They start with a physically-motivated functional form for $E(T)$ and seek to find the most likely curve of the infinitely many curves which optimize some likelihood function such as χ^2 . In reality, the functional

form of the energy is not known. What is known is that finite temperatures spread the excitation spectrum of a quantum system. The question one might like to ask, “what is the curve that fits the data” is therefore ill-defined. Without additional regularization, an infinite number of curves fit the data and, unless the precise functional form of the internal energy $E(T)$ is known, there is no precise answer to this question. However, if we know the form of the thermal blurring function $K(\beta, \omega)$, we may ask the question, “given the blurring function and any other relevant prior information that we know, what is the most probable spectrum $\rho(\omega)$ from which this energy data $E(T)$ might arise?” As discussed in detail below, this is the precise question that the MEM answers.

In addition to relying on fundamental properties of quantum systems instead of a functional form, further benefits also accrue from employing our MEM technique. For example, since the MEM gives errorbars on integrated quantities, the uncertainties in both $E(T)$ and $C(T)$ are known when obtained via our MEM technique. Other advantages of our technique will be discussed below. Before discussing algorithmic details, it is useful and instructive to briefly review the MEM.

IV. THE MAXIMUM ENTROPY METHOD

The Maximum Entropy Method (MEM) is discussed in detail elsewhere. [5,7–9] Here, we wish to review only as much of the MEM as is necessary to understand the new technique.

The MEM is frequently used to analytically continue QMC imaginary-time Green Function data to real frequencies. [5] However, it is a general technique that is not limited to analytic continuation or to QMC-related problems. In fact, the MEM has a relatively long history as an image reconstruction technique in photography and dynamic light scattering problems. [10,7]

In such problems, the observed image is the result of Gaussian blurring of light transmitted from a source through a medium, such as the atmosphere. Hence, the functional form of the image is not known and the question of whether the observed data fits a specific functional form is ill-defined – there are an infinite number of curves that fit the data! Instead, the best that one can do is to seek the *most probable* image given the data. This is exactly what the MEM sets out to accomplish.

This is done using Bayesian statistics. If there are two events, a and b , then by Bayes’ theorem, the joint probability of these two events is

$$P(a, b) = P(a|b)P(b) = P(b|a)P(a), \quad (8)$$

where $P(a|b)$ is the conditional probability of a given b . The probabilities are normalized so that

$$P(a) = \int db P(a, b) \text{ and } \int da P(a) = 1. \quad (9)$$

In our problem, we search for the spectrum ρ which maximizes the conditional probability of ρ given the data E ,

$$P(\rho|E) = P(E|\rho)P(\rho)/P(E). \quad (10)$$

Typically, one calls $P(E|\rho)$ the likelihood function and $P(\rho)$ the prior probability of ρ (or the prior). Since we work with one set of QMC data at a time, $P(E)$ is a constant during this procedure and may be ignored. The prior and the likelihood functions require more thought, and are discussed in detail in Ref. [5], here we present the salient results of that discussion.

If the spectrum is positive-definite, we may think of it as a un-normalized probability density:

$$\int_{-\infty}^{\infty} d\omega \rho(\omega) < \infty. \quad (11)$$

Then by Skilling, [8] the prior probability is proportional to $\exp(\alpha S)$ where S is the entropy defined relative to some positive-definite function $m(\omega)$

$$S = \int_{-\infty}^{\infty} d\omega [\rho(\omega) - m(\omega) - \rho(\omega) \ln(\rho(\omega)/m(\omega))], \quad (12)$$

and

$$P(\rho) \propto P(\rho|m, \alpha) \propto \exp(\alpha S), \quad (13)$$

where $m(\omega)$ is the default model since in the absence of data $\rho = m$. Selection of the default model for this method is discussed in Sec. V. The other unknown quantity α is determined during the MEM to maximize the probability of the image ρ given the data.

The likelihood function follows from the central limit theorem. If each of the measurements $E_{i,T}$ ($E_T \equiv E(T)$) of the energy at a specific temperature T is independent, then in the limit of a large number of measurements N_d to determine each E_T the distribution of the E_T becomes Gaussian. The probability of measuring a particular E_T is

$$P(E_T) = \frac{1}{\sqrt{2\pi\sigma_T^2}} \exp \left[-\frac{1}{\sigma_T^2} (\langle E_T \rangle - E_T)^2 / 2 \right], \quad (14)$$

with an error estimate given by

$$\sigma_T^2 = \frac{1}{N_d(N_d - 1)} \sum_i (\langle E_T \rangle - E_{i,T})^2 \quad (15)$$

and

$$\langle E_T \rangle = \frac{1}{N_d} \sum_{i=1}^{N_d} E_{i,T} \quad (16)$$

for the N_d measurements of $E_{i,T}$ at temperature T .

Then the likelihood function $P(E|\rho)$ of measuring the set of E for a given image ρ is

$$P(E|\rho) \propto e^{-\chi^2/2} \quad (17)$$

where

$$\chi^2 = \sum_T^{\text{all}T} \frac{(E_T - \sum_{\omega} \omega K(\omega, T) \rho(\omega))^2}{\sigma_T^2} \quad (18)$$

and we have discretized the integral Eq. 6.

We are now in a position to perform the MEM and find the most probable image ρ given the data E_T . We wish to maximize the joint probability of the image or weight ρ given the data E ; the default model m ; and the Lagrange multiplier α

$$\begin{aligned} P(\rho|E, m, \alpha) &\propto P(E|\rho)P(\rho|m, \alpha) \\ &= \frac{\exp(\alpha S - \chi^2/2)}{Z_S Z_L} \end{aligned} \quad (19)$$

where Z_S and Z_L are normalization factors, independent of the image. For a fixed α and the given data E , the most probable image $\hat{\rho}(\alpha)$ is the one that maximizes $Q = \alpha S - \chi^2/2$. This may be found, for example, using Newton's method.

The details of implementing a MEM code and finding α are given elsewhere. [5] We will not repeat that presentation here. A MEM code written according to Ref. [5] is recommended for performing the technique we discuss herein. [11] Having discussed the general MEM formalism, we now turn to the specific algorithmic details of our new technique.

V. ALGORITHMIC DETAILS OF THE NEW TECHNIQUE

We desire to express the internal energy of the system as an integral over a density of energy levels times a relation between energy and temperature, according to Eq. 6. To that end, we make the following Ansatz

$$E(T) = - \int_{-\infty}^{\infty} d\omega \omega [F(\beta, \omega) \rho_F(\omega) + B(\beta, \omega) \rho_B(\omega)], \quad (20)$$

where F and B are the Fermi- and Bose-distribution functions, respectively

$$\begin{aligned} F(\beta, \omega) &= \frac{1}{1 + e^{\beta\omega}} \\ B(\beta, \omega) &= \frac{1}{1 - e^{\beta\omega}} \end{aligned} \quad (21)$$

for $\beta = 1/T$ (we have set the Boltzmann constant equal to unity $k_B = 1$).

This Ansatz corresponds roughly to describing the energetics of the system as consisting of separate linear contributions from Fermi- and Bose-excitations and

imposes the constraint that the corresponding energy $E(T)$ increases monotonically with temperature T so that $C(T) \geq 0$. In addition, since the degeneracy of the ground state and the total number of accessible states is generally known, the infinite temperature entropy is generally known. S_{∞} may be obtained from

$$S_{\infty} = - \int_0^{\infty} \frac{dT}{T} \int_{-\infty}^{\infty} d\omega \omega \left[\frac{\partial F}{\partial T} \rho_F(\omega) + \frac{\partial B}{\partial T} \rho_B(\omega) \right] \quad (22)$$

by noting that the temperature integral for the Fermi term can be done analytically and since $\rho_B(\omega)$ is odd the Bose term does not contribute to the integral. [17] The net result is that

$$S_{\infty} = \ln 2 \int_{-\infty}^{\infty} d\omega \rho_F(\omega) \quad (23)$$

Additional information such as this may be imposed by modifying the prior or the likelihood function. Given the similarity of Eq. 23 and Eq. 20, which appears as part of the likelihood function, we choose the latter approach. We introduce S_{∞} as an additional datum with a relative error estimate σ_S/S_{∞} chosen to be approximately equal to the smallest relative error estimate of the energy data. We discuss our reasons for choosing this Ansatz in the appendix.

With this Ansatz, we are in a position to employ the MEM. We write $K\rho$ from Eq. 6 as a linear combination of $F\rho_F + B\rho_B$. Eq. 18 for χ^2 is modified similarly. We pick the default model in the following manner. We note first that it must be positive definite and integrable. We employ a Gaussian default model, which satisfies these criteria.

Once the default model is selected, the method described in Ref. [5] may be applied straight away. To further illustrate the method, we now apply it to a non-trivial model.

VI. EXAMPLE: 3D PERIODIC ANDERSON MODEL

The 3d Periodic Anderson Model (PAM) is often used to investigate f-electron systems, where electronic correlations are important for the phenomena under study. It is a simplified lattice model in which the Coulomb interaction is limited in range to on-site interactions only and then only within one of the two bands. Nevertheless, it is a rich model in which the interplay between delocalization (kinetic energy), Coulomb repulsion, Pauli exclusion, temperature, and electron density give rise to a wide variety of phenomena.

The periodic Anderson Hamiltonian is

$$\begin{aligned} H = & \sum_{k\sigma} \epsilon_k d_{k\sigma}^{\dagger} d_{k\sigma} + \sum_{k\sigma} V_k (d_{k\sigma}^{\dagger} f_{k\sigma} + f_{k\sigma}^{\dagger} d_{k\sigma}) \\ & + U_f \sum_i (n_{if\uparrow} - \frac{1}{2})(n_{if\downarrow} - \frac{1}{2}) \end{aligned}$$

$$+ \sum_{i\sigma} \epsilon_f n_{if\sigma} - \mu \sum_{i\sigma} (n_{if\sigma} + n_{id\sigma}). \quad (24)$$

We choose a simple cubic structure for which,

$$\epsilon_k = -2t_{dd} [\cos k_x a + \cos k_y a + \cos k_z a], \\ V_k = -2t_{fd} [\cos k_x a + \cos k_y a + \cos k_z a], \quad (25)$$

where a is the lattice constant. The dispersion of V_k reflects our choice of near-neighbor (as opposed to on-site) hybridization of the f and d electrons. With on-site hybridization, the PAM is an insulator at half-filling, whereas with our intersite hybridization choice the half-filled, symmetric PAM is metallic.

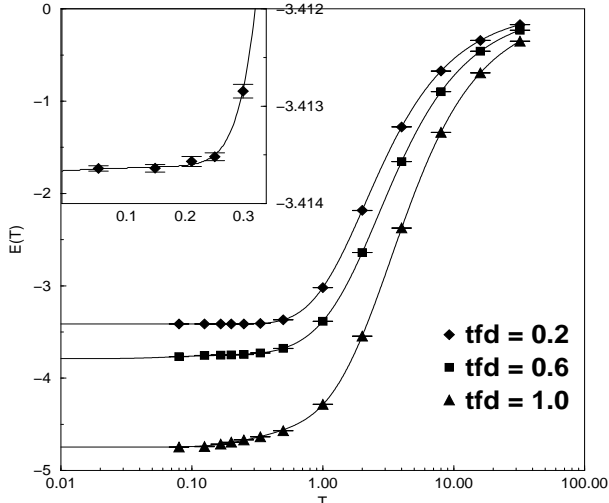


FIG. 1. Energy vs. temperature for various $f-d$ hybridizations t_{fd} . The symbols mark QMC data, with errorbars. The solid lines mark the energy obtained via the MEM. There is an excellent agreement between the data and the MEM results throughout the range of temperatures. This is further illustrated in the inset, where a magnified view of the lowest QMC temperature values for $t_{fd} = 0.2$ is shown.

The parameter values and the temperature T in this work are given in units of t_{dd} . We take $U_f = 6$ and explore a range of t_{fd} and T values. QMC results for this model were obtained using the determinant algorithm, [12] which provides an exact treatment (to within statistical errors and finite size effects) of the correlations. We further choose the symmetric PAM ($\mu = \epsilon_f = 0$, and thus half-filling: $\langle n_{if} \rangle = \langle n_{id} \rangle = 1$) in order to eliminate the QMC “sign problem,” allowing accurate simulations at low temperatures.

This version of the PAM has been studied in this parameter regime and is known to undergo a sharp finite-temperature crossover at finite $t_{fd} \approx 0.6 - 0.8$ with an associated, abrupt change in the free energy which is reflected in the specific heat. [4,3] These thermodynamic anomalies are believed to be signals of a zero-temperature metal-insulator phase transition in the f -band which is

also seen as a finite-temperature crossover to a localized f -electron system. [13,14] We will test our new technique by using it to reproduce the published work.

Figure 1 shows the energy obtained via the MEM using Eq. 20 for various hybridizations $t_{fd} = 0.2, 0.6, 1.0$ along with QMC data and errorbars on the QMC data. There is an excellent agreement between the QMC data and the MEM results throughout the range of temperatures simulated by QMC. The quality of the agreement is further illustrated by the inset in Fig. 1, which shows a magnified view of the lowest QMC temperature values for $t_{fd} = 0.2$.

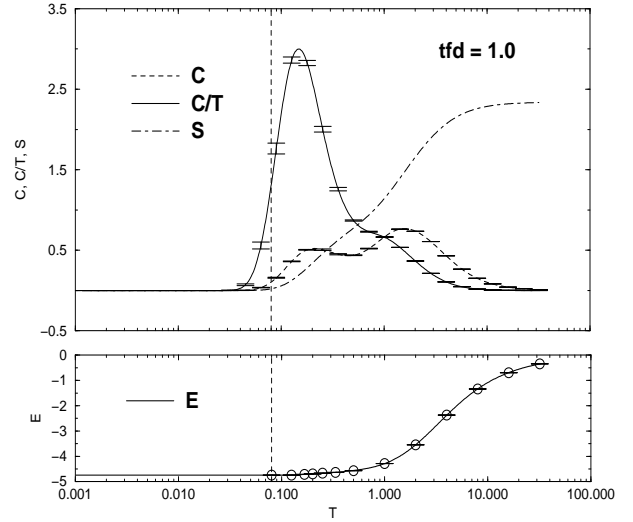


FIG. 2. Specific heat $C(T)$, specific heat divided by temperature $C(T)/T$, and entropy $S(T)$ (top figure), and energy $E(T)$ (bottom figure) as a function of temperature T for a fixed hybridization $t_{fd} = 1.0$. Representative error bars are shown. The dashed vertical line at $T = 0.08$ corresponds to the lowest QMC data point. A peak in $C(T)/T$ appears at $T \approx 0.15$ due to singlet formation. At a higher temperature, a hump appears in $C(T)/T$ which is believed to be due to the suppression of charge fluctuations. The total entropy $3.375 \ln 2$ in the system obtained by integrating the image from the MEM (see the text) matches both the total entropy obtained from integrating $C(T)/T$ (Eq. 4) and the value of $S_\infty = 4 \ln 2 - S_0$ known for the model.

Once one obtains the image, the specific heat $C(T)$ is obtained by differentiating as in Eq. 1. Fig. 2 shows the specific heat $C(T)$, the specific heat divided by the temperature $C(T)/T$, and the entropy $S(T)$ in the top figure as a function of temperature T for a fixed hybridization $t_{fd} = 1.0$. For comparison, the bottom figure shows the energy $E(T)$. At this hybridization, singlets are known to form at low temperatures. [4,3] This is reflected in a peak in $C(T)/T$ appearing at $T \approx 0.15$. The singlet formation peak is also visible in $C(T)$. A smaller peak in $C(T)$ at higher temperatures is believed to be due to the suppression of charge fluctuations in the f -band.

The entropy may be found in two ways. First, $S(T)$ may be obtained by integrating $C(T)/T$ according to Eq. 2. This was done and is plotted in Fig. 2. The entropy found in this manner saturates at high temperatures at the infinite-temperature limit $S_\infty = 4 \ln 2 - S_0$ known for this model. [3] Second, the infinite temperature entropy may calculated by integrating ρ_F , Eq. 23. The latter estimate is $S_\infty = 3.375 \ln 2$, which is also that obtained from integrating $C(T)/T$ (Eq. 4) and the value of $S_\infty = 4 \ln 2 - S_0$ known for the model.

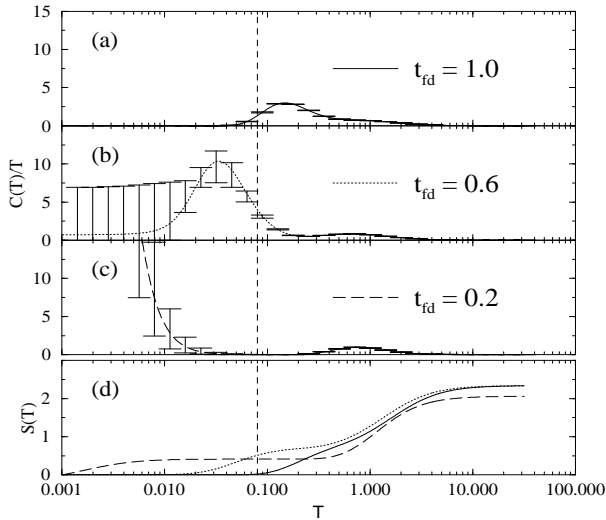


FIG. 3. Specific heat divided by temperature $C(T)/T$ for various $f - d$ hybridizations t_{fd} , (a) $t_{fd} = 1.0$, (b) $t_{fd} = 0.6$, and (c) $t_{fd} = 0.2$. The corresponding entropies from integrating $C(T)/T$ (Eq. 4) are shown in panel (d). The dashed vertical line at $T = 0.08$ corresponds to the lowest QMC data point. At large hybridizations, $t_{fd} = 1.0$, essentially all of the entropy in the system is quenched within the temperatures accessed by the simulations (a). As the hybridization decreases, antiferromagnetic ordering at temperatures below those accessed by the simulations becomes important and a substantial amount of entropy is not quenched within the simulated temperatures. The sum rule enforces the total entropy in the system, which appears in the results below the accessed temperatures, yet the most probable form of the specific heat for this regime cannot be precisely determined. This is reflected in large errorbars seen in panels (b) and (c) for the specific heat at temperatures below those accessed by the simulations.

In addition to singlet formation at low temperatures for relatively large hybridizations t_{fd} , the metallic PAM develops antiferromagnetic long-range-order (AFLRO) at low temperatures for small t_{fd} . Hence, if one examines $C(T)/T$ for decreasing hybridization t_{fd} , the singlet-formation peak should eventually disappear and a low-temperature peak corresponding to AFLRO should appear in $C(T)/T$. Previous work has observed the disappearance of the singlet-formation peak, but did not access a sufficiently low temperature to observe the appearance of the AFLRO peak. [3]

Figure 3 shows the specific heat divided by temperature $C(T)/T$ for various $f - d$ hybridizations t_{fd} , (a) $t_{fd} = 1.0$, (b) $t_{fd} = 0.6$, and (c) $t_{fd} = 0.2$. The corresponding entropies from integrating $C(T)/T$ (Eq. 4) are shown in panel (d). Here, we observe the disappearance of the singlet peak with decreasing hybridization t_{fd} . At $t_{fd} = 1.0$ there is a substantial singlet formation peak. At $t_{fd} = 0.2$ there is no singlet formation for any temperature accessed by the simulations, and possibly no singlet formation even at $T = 0$. [13] The intermediate hybridization $t_{fd} = 0.6$ corresponds to a regime where singlet formation occurs suddenly for low temperatures, [4] as is reflected in the shift of the singlet peak to lower temperatures in Fig 3.

The sum rule [15]

$$S_\infty = 4 \ln 2 - S_0 \quad (26)$$

for the entropy enforces the total entropy in the system. This is an important feature of the method and satisfying the sum rule is one check on whether the specific heat is physically reasonable. However, when the system does not quench all of the entropy by the lowest temperature accessed by the QMC simulation, one may worry whether enforcing the sum rule will push spurious entropy into the specific heat. This does not happen, as shown in Fig. 3(d). Instead, this entropy beyond that quenched within the accessed temperatures goes below the lowest QMC temperature, where indeed it should go on physical grounds. However, then the extrapolation below the lowest QMC data point is unreliable. This unreliability of the extrapolation to a regime where the sum rule has forced entropy below the QMC data is seen by the large error bars on the specific heat in this extrapolation regime. That is, the method puts the entropy where it belongs, but then informs one that the results of the MEM in this regime are totally uncertain. This is an extremely desirable result. [16]

VII. SUMMARY

We have described a novel technique to obtain the internal energy as a function of temperature, as well as the specific heat, the entropy, and the free energy of a system using QMC energy data sampled at a small, finite set of temperature values. Our technique relies on probability theory to obtain the *most probable* thermodynamic functions given the sampled QMC energy. The question of determining the number of fitting parameters, which plagues the other methods, is thereby removed. An entropy sum rule or other appropriate *a priori* information may also be used, if known. The technique was illustrated by applying it to the 3d Periodic Anderson Model. An important benefit of the technique is that it returns not

only the thermodynamic functions, but also their uncertainties. This is a significant improvement over the prior techniques.

ACKNOWLEDGEMENTS

We are grateful to J.E. Gubernatis, A.K. McMahan, R.T. Scalettar, and R.N. Silver for helpful discussions. This work was supported by NSF grants DMR-9704021 and DMR-9357199. The QMC simulations were performed on the U.S. Department of Energy ASCI Red and Blue-Pacific computers.

APPENDIX A: THE FORM OF THE ENERGY ANSATZ

In section V we wrote the Ansatz for the energy as

$$E(T) = - \int_{-\infty}^{\infty} d\omega \omega F(\beta, \omega) \rho_F(\omega) - \int_{-\infty}^{\infty} d\omega \omega B(\beta, \omega) \rho_B(\omega), \quad (\text{A1})$$

where F and B are the Fermi- and Bose-distribution functions, respectively

$$F(\beta, \omega) = \frac{1}{1 + e^{\beta\omega}} \quad (\text{A2})$$

$$B(\beta, \omega) = \frac{1}{1 - e^{\beta\omega}}.$$

Each integral in A1 is a Fredholm integral equation of the first kind for the corresponding density with either F or B as the kernel. Since these kernels are continuous, the problem of inverting Eq. A1 to find $E(T)$ is ill-posed [18] and must be regularized. MEM provides an efficient regularization method. In this appendix we motivate our Ansatz and discuss other possible functional forms.

The Ansatz given in Eq. A1 is not the only possible, or even sensible choice. In general one wants to choose as an Ansatz the one that captures the underlying physics of the problem. For models such as the PAM, we expect a density of Fermionic excitations represented by ρ_F associated with quasiparticle excitations. Since quasiparticles are conserved, their density should be positive definite which is required when the MEM formalism is employed.

In addition, we expect a density ρ_B of Bosonic excitations associated with collective behavior such as spin waves. With no Bosonic operators in the Hamiltonian, these Bosons are not conserved and have zero chemical potential. Thus, $\rho_B(\omega > 0) > 0$ corresponding to the creation of such excitations, and $\rho_B(\omega < 0) < 0$ corresponding to their destruction. This choice of ρ_F , ρ_B , and K constrain the specific heat $C(T)$ to be positive definite, $C(T) \geq 0$. Furthermore, $\rho_B(\omega)$ is odd as required by the

Fluctuation-Dissipation theorem. Therefore, we may reduce the second integral in Eq. A1 to the range $(0, \infty)$ where $\rho_B(\omega)$ is positive semi-definite.

An Ansatz should also provide a faithful representation of the $E(T)$ data. To explore this question, we note that for a finite-sized system $E(T)$ is an analytic function that can be expanded in a Taylor series in T around $T = 0$. Expanding $F(\beta, \omega)$ in a Sommerfeld low temperature expansion [19] yields only even powers of T in the energy. In order to get odd powers of T that complete the Taylor series, the Bosonic kernel is required. Having the Taylor expansion for $E(T)$, the remaining question is the positive-definite nature of the image $\rho(\omega)$. Even the fact that the energy is monotonic does not yield a mathematical constraint that ρ_F and $\rho_B(\omega > 0)$ are positive definite, yet in practice this constraint imposed by the MEM is not a limitation.

It is possible to dispose of the Ansatz and use a general form for the energy. A faithful representation for systems in thermal equilibrium with a heat bath is provided by

$$E(T) = - \frac{\int_{-\infty}^{\infty} d\omega \omega \rho(\omega) \exp(-\omega/T)}{\int_{-\infty}^{\infty} d\omega \rho(\omega) \exp(-\omega/T)} \quad (\text{A3})$$

where $\rho(\omega) > 0$ is the density of eigenstates of the Hamiltonian. However, since the relationship between the density and E is non-linear, the MEM algorithm described in Sec. IV cannot be applied without significant modification. Furthermore, the representation provided by Eq. A1 in each case we have tested has provided a fit to within the measured error. Thus, the additional complications associated with the use of Eq. A3 seem unnecessary for this and similar systems. However, this general technique would allow extension of the method to Classical Monte Carlo simulations and is something we are currently exploring.

- [1] R. Fye and R. Scalettar, Phys. Rev. **B 36**, 3833 (1987).
- [2] D. Duffy and A. Moreo, Phys. Rev. **B 55**, 12918, (1996).
- [3] A.K. McMahan, *et. al.*, J. Comput.-Aided Mater. Design **5**, 131 (1998).
- [4] C. Huscroft, *et. al.*, Phys. Rev. Lett. **82**, 2342 (1999).
- [5] M. Jarrell and J.E. Gubernatis, Phys. Rep. **269**, 135 (1996).
- [6] We are currently investigating the appropriate blurring function for classical systems as well as the development of a generally applicable MEM method for obtaining thermodynamic properties from classical systems via Monte Carlo. (See, Appendix A.)
- [7] R.K. Bryan, Eur. Biophysics J. **18**, 165 (1990).
- [8] J. Skilling, in *Maximum Entropy and Bayesian Methods*, edited by J. Skilling (Kluwer Academic, Dordrecht, 1989).
- [9] M. Jarrell, *et. al.*, Phys. Rev. **B 44**, 5347 (1991).

- [10] W.H. Press, *et. al*, *Numerical Recipes in C* (Cambridge, 2d ed., 1992), p. 818.
- [11] However, we note that the energy data $E(T)$ are uncorrelated, so the re-binning technique discussed in Ref. [5] does not apply here.
- [12] R. Blankenbecler *et.al*, Phys. Rev. **D24**, 2278 (1981).
- [13] K. Majumdar, *et. al*, unpublished.
- [14] K. Held, *et. al*, unpublished (cond-mat/9905011).
- [15] The constant $S_0 = (2N_0/N) \ln 2$ where N is the total number of lattice sites and N_0 is the number of discrete k points which have $\epsilon_k = V_k = 0$ on a finite lattice. [3]
- [16] The entropy $S(T)$ for $t_{fd} = 0.2$ shown in Fig. 3 does not saturate to the total entropy in the system. This is not a violation of the sum rule. The MEM results were not run to a sufficiently low temperature to capture all of the entropy via Eq. 2. When S_∞ is obtained by integrating the image (Eq. 23) the sum rule is found to be satisfied.
- [17] As discussed, the MEM yields the most probable image, $\rho_F(\omega)$ and $\rho_B(\omega)$. For the QMC data studied, we find no finite Bose contributions to the image, however.
- [18] R. Kress, *Linear Integral Equations* (Springer, 2d ed., 1999), p. 265.
- [19] R. Balescu, *Equilibrium and Non-equilibrium Statistical Mechanics* (Wiley, 1975), p. 173.